Molecular Crystals and Liquid Crystals Science and Technology. Section A. Molecular Crystals and Liquid Crystals

Publication details, including instructions for authors and subscription information:
http://www.tandfonline.com/loi/gmcl19

Dynamical Director Profile Analysis of Ferroelectric Liquid Crystals using Modulated Wave-guide Spectroscopy

A. Fahrwald [a], N. Klöpper [a], S. Ito [a], F. Kremer [a] & Th. M. Fischer [a]

[a] Fakultät für Physik, Universität Leipzig, Linnéstr. 5, 04103, Leipzig, Germany

Version of record first published: 24 Sep 2006

To cite this article: A. Fahrwald, N. Klöpper, S. Ito, F. Kremer & Th. M. Fischer (1998): Dynamical Director Profile Analysis of Ferroelectric Liquid Crystals using Modulated Wave-guide Spectroscopy, Molecular Crystals and Liquid Crystals Science and Technology. Section A. Molecular Crystals and Liquid Crystals, 325:1, 173-183

To link to this article: http://dx.doi.org/10.1080/10587259808025393

Mol. Cryst. Liq. Cryst., Vol. 325, pp. 173–183
Reprints available directly from the publisher
Photocopying permitted by license only

Dynamical Director Profile Analysis of Ferroelectric Liquid Crystals using Modulated Wave-guide Spectroscopy

A. FAHRWALD*, N. KLÖPPER, S. ITO, F. KREMER and TH. M. FISCHER

Fakultät für Physik, Universität Leipzig, Linnéstr. 5, 04103 Leipzig, Germany

(Received 28 January 1998; In final form 1 May 1998)

The dynamic director profile of a ferroelectric liquid crystal (FLC) throughout a surface stabilized liquid crystalline cell is measured using modulated wave-guide spectroscopy. It is shown that the ferroelectric switching in the center of the cell and the non switching surface boundary layers are well resolved with respect to their thickness and orientation dynamics.

Keywords: Liquid crystal; wave-guide spectroscopy; boundary layer

INTRODUCTION

Guided wave spectroscopy is a powerful tool for the study of various details of the director profile of liquid crystals within surface stabilized cells [1]. The guided modes have different distributions of the light intensity along the normal of the cell. The reflectivity data obtained from each mode is sensitive to the director orientation at the location of the intensity maxima and the orientation at various distances from the surface boundary can be remodeled. The technique has been used to determine the static director profile of ferroelectric liquid crystals in order to decide on the validity of various models proposed in the Ref. [2]. This technique has been improved using half leaky guided waves and various complicated structures could be unraveled [3–5].

* Corresponding author.

Ito *et al.* [6] have extended the non leaky wave-guide technique for phase sensitive measurements of dynamic reorientation processes by modulating the ferroelectric liquid crystal cell with alternating electric fields. Using time resolved optical wave-guide spectroscopy the transient behavior of nematic [7] as well as of ferroelectric [8] liquid crystals was determined with a microsecond resolution. However, the power of the technique, lying especially in the ability of resolving the orientation-profile, so far has not been demonstrated for the modulated or time resolved wave-guide spectroscopy.

Using depolarized total internal reflection technique it was shown [9], that a rubbed-polymer surface orients the interfacial director of a chiral smectic liquid crystal parallel to the surface and along the rubbing direction even though this orientation is off from the bulk smectic C^* tilt cone. By application of an electrical field the director at the surface switches irreversibly onto the tilt cone away from the rubbing direction.

It is the purpose of this paper to show that similar resolution of the dynamic director profile is possible with modulated dynamical wave-guide spectroscopy. We will show that different dynamics is observed in the boundary layers reaching out 0.14 micrometers from the cell surfaces compared to the inner part of the cell.

EXPERIMENT

The experimental setup of the optical wave-guide spectrometer is shown in Figure 1. The electric field modulated reflectivity of the sample cell is recorded as a function of the angle of incidence for *p* and *s* polarized light respectively.

A He–Ne laser $\lambda = 632.8$ nm is used as the light source. A quarter-wave plate in conjunction with a polarizer enables the generation of linear polarized light of arbitrary direction with defined intensity. After being reflected from the prism coupled sample cell, the modulated light passes an analyzer and hits the detector. The modulation of the signal is then recorded with a lock in amplifier (SR 830 Stanford Research). The sample is mounted on a $\vartheta - 2\vartheta$ goniometer allowing to scan incident angles from 10 to 90 degrees. For fixed orientation of the liquid crystal in the sample cell, wave-guide modes are excited at defined incident angles. At these wave-guide resonance angles there is a drop in reflectivity. The light couples into the liquid crystalline cell and propagates between the gold covered glass plates surrounding the liquid crystal. As the ferroelectric liquid crystal experiences

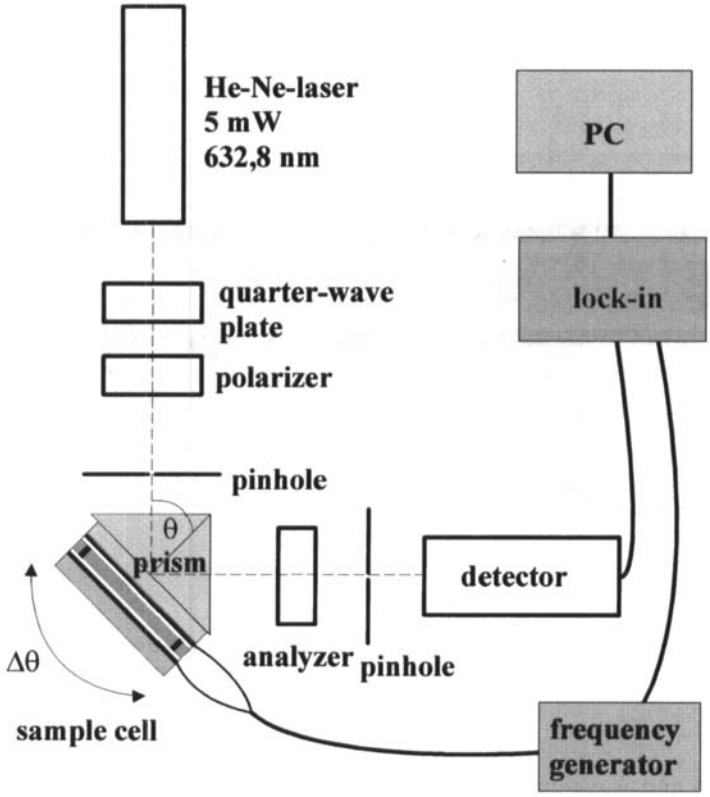

FIGURE 1 Schematic representation of the experimental setup of the wave-guide spectrometer.

an AC-electric field the orientation is modulated and so is the reflectivity of the sample. The modulated reflectivity as a function of the incident angle enables us to determine the reorientational dynamics of the ferroelectric liquid crystal within the cell.

The sample cell (Fig. 2) has a seven layer structure. A thin gold cladding layer is evaporated on two glass slides (BK7). Both gold layers build up the resonance cavity for the wave-guide modes and they serve as electrodes for the modulated electric fields to be applied. To induce a planar orientation of the liquid crystal the surfaces are covered with rubbed polyimide layers. Subsequently the thickness of the cell is fixed using PET-spacer (3 – 6 μm). A 90 degree prism (BK7) is attached to the front side of the cell using image matching oil. In-between all steps the thickness of the gold and polyimide layers as well as the spacing of the empty cell are determined from surface

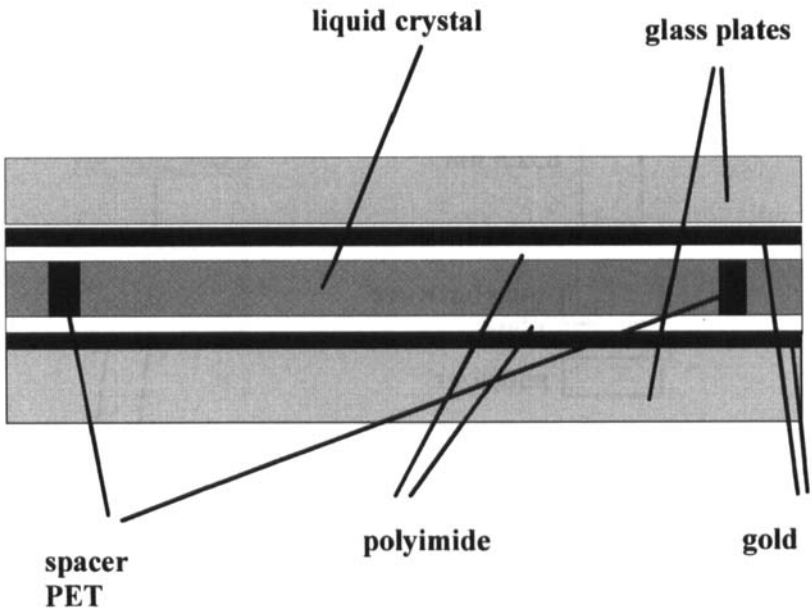

FIGURE 2 Schematic structure of the liquid crystalline cell used. The thickness of each layer is listed in Table I. The rubbing direction of one polyimide layer is parallel to the other.

plasmon and wave-guide resonances by performing static reflectivity scans of the subsequent parts of the cell respectively. The whole sample is placed in a temperature controlled sampleholder with a precision of 0.1 K. The cell is filled with the commercial ferroelectric liquid crystalline mixture ZLI 4237-100 (Merck). The phase sequence is: −20°C - SmC* − 61°C - SmA − 73°C - Ch − 83°C - iso. Homogeneous alignment is obtained by heating and cooling across the SmC*−SmA phase transition during simultaneous application of an AC-field (2×10^4 V/cm, 20 Hz). All experiments presented are carried out in the SmC* phase at a temperature of 55°C.

For frequencies well below the switching time the bistability of the ferroelectric switching leads to a square wave signal of the reflectivity as a function of time. In this regime the response $R(f)$ measured on the first harmonic f of the electric field modulation can be simply expressed as the difference in reflectivity R of both bistable orientations of the liquid crystal

$$R(f) = 2/\pi(R(+E) - R(-E))$$

where $+E$ and $-E$ denotes the electric field.

RESULTS

The oriented liquid crystal forms the bookshelf structure in the SmA-phase. It has been shown by Pelzl [10]; Rieker [11] and Elston [2], that in the SmC* - phase the director twists away from the rubbing direction by an angle δ, with zero tilt of the director to the plane defined by the cell surface. This structure is consistent with the Chevron model [11], where the smectic layers are tilted with a layer kink in the middle of the cell. Using other techniques [12] it could be also shown, that this model breaks down in the vicinity (approximately 100 nm) of the cell surface and that some other structure is adopted in these boundary layers. These boundary layers have been resolved with half leaky wave-guide spectroscopy [3, 4, 13]. With dynamical wave-guide spectroscopy the dynamics of these boundary layers can be measured. In our setup we turned our cell such that the orientation of the director of the Chevron structure adopted at negative electric field coincided with the plane of incidence of the laser beam. This was done by minimizing the p to s conversion.

After this an AC-electric field ($E = 1.3 \times 10^4$ V/cm, $f = 2$ kHz) has been applied allowing to record directly the difference of reflectivity of the orientations obtained for the electric fields of opposite direction. Figure 3 shows a modulated spectrum of the ferroelectric liquid crystals for (a) s polarized and (b) p polarized light. For frequencies lower than the typical Goldstone mode relaxation rate the dynamical reflectivity is simply the difference of the two reflectivities for the director profiles of the two stable orientations *i.e.*,

$$r_{AC}(\vartheta) = 2/\pi(r_E(\vartheta) - r_{-E}(\vartheta)).$$

The timedependent reflectivity signal produced by positive electric field is in phase with the applied voltage and the wave-guide resonances corresponding to the orientation at positive electric field can be seen as dips in the Fourier transformed modulated reflectivity curve. In contrary to this the contributions from negative electric field being 180 degrees out of phase show up as peaks in the Fourier transformed signal. The director for positive electric field makes a twist angle with the plane of incidence twice the amount of twist of the plane of incidence from the projection of the cone axis onto the sample plane. No special symmetry is associated with this configuration. Consequently there is strong coupling between p and s polarized light and the same wave-guide modes may be excited with p or s polarized light. It can be seen from Figure 3 that all wave-guide modes (*i.e.*,

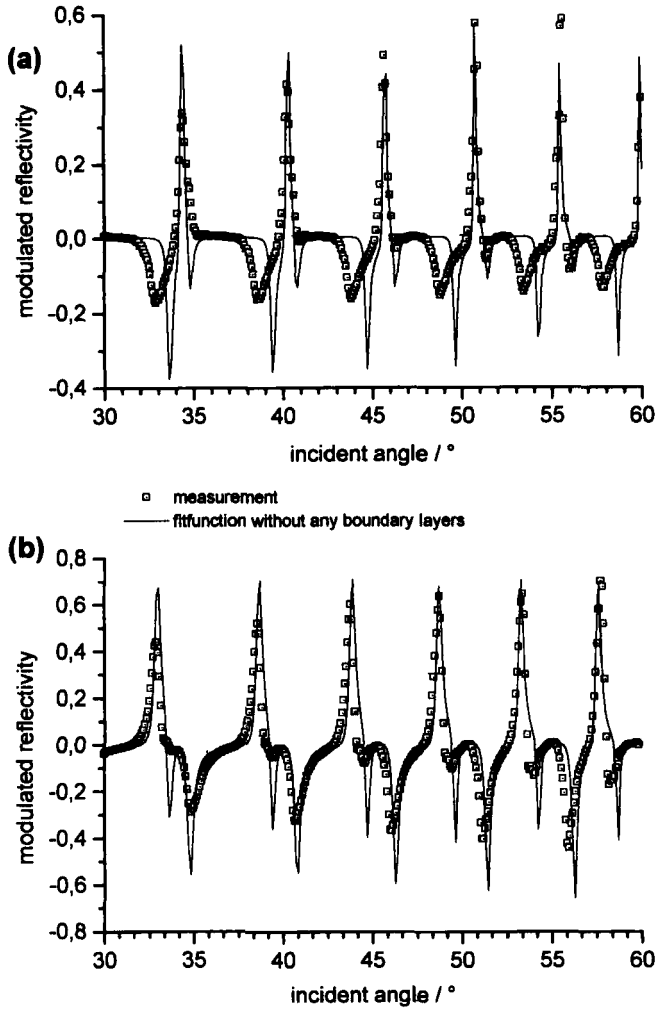

FIGURE 3 The modulated reflectivity scan measured in the 1st harmonic of the applied field as a function of angle of incidence for (a) *s*- and (b) *p*-polarized incident light ($\lambda = 632.8$ nm) in the Smectic C* phase ($T = 55°C$). The best fitfunction without any surface layer are shown as solid lines. The fitting parameters are listed in Table I. The twist angle is 9.5 degree.

dips in the modulated spectra) are excited for both *p* and *s* polarized light. The contribution to the dynamic spectrum from negative electric fields (the peaks in Fig. 3) show a quite different behavior. The director during this half period coincides with the plane of incidence. Consequently for symmetry reasons *p* and *s* polarized light do not couple. Only half of the wave-guide modes excited at positive field are excited at negative field, one half by *p*

polarization the other half by *s* polarization. Therefore without fitting any data one can determine the twist of the director.

We now tried to fit the data shown in Figure 3 using two models. One relying on the Chevron structure without any boundary layers. In this model the whole director profile uniformly switches between the states, where the director is twisted to the right and left (Fig. 4a). The dielectric constant of the liquid crystal layer and the twist angle were used as fitting parameters. As the thickness of the cell usually changes after filling of the cell it was used as fitparameter as well, however the deviation of the fitted thickness from the thickness of the unfilled cell always was smaller than 50 nm. Both, *p* and *s* reflectivities were fitted simultaneously. The best fit obtained using this homogeneous reorientation process ($\delta = 9.5°$, $\varepsilon_{\parallel} = 2.06$, $\varepsilon_{\perp} = 2.53$) is shown

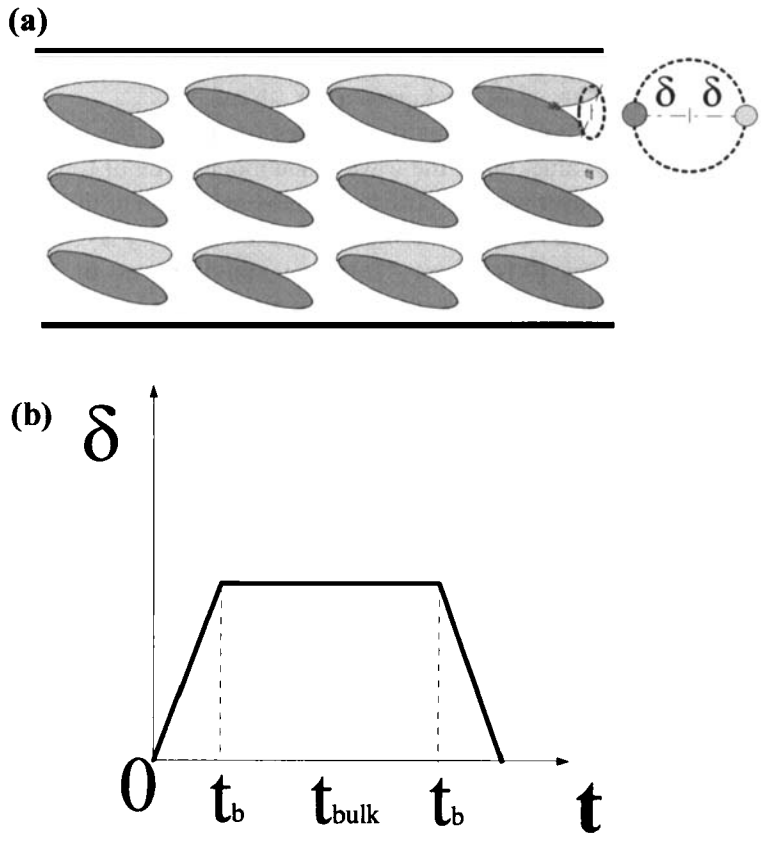

FIGURE 4 (a) Uniform switching model which used for the fitting results in Figure 3; (b) Twist angle profile for the increasing twist angle boundary layer model.

in Figure 3 as solid lines. The fit obtained describes the qualitative behavior of the wave-guide resonances quite well, however it was not possible to fit all the resonance positions for negative and positive electric field and for both polarizations simultaneously. It was possible to obtain fits of similar quality using somewhat different fitting parameters, but the resonances never matched the values measured in the experiment. Since no better fit could be obtained using the model of homogeneous reorientation one can deduce, that the reorientational behavior is more complex. It has been mentioned by Elston [2], that the Chevron model breaks down in the vicinity of the surface of the cell. Deviations of this model in the vicinity of the cell surfaces have been proposed in order to explain the white light transmission data between crossed polarizers. These boundary layers are believed to be approximately 0.1 μm thick, with the twist of the director changing gradually from zero degree to the twist present in the Chevron structure or some other complex structure. The switching of the director in the boundary layers therefore is suppressed compared to the interior of the cell. We tried to model these boundary layers by layers of thickness t_b(Fig. 4b).

The director orientation gradually increases from zero twist at the cell surface to the bulk value. Since the wave-guide modes are not too sensitive to the details of the layer we arbitrarily fixed one orientation to the projected cone axis. The thickness and the twist angle of the boundary layer was used as fitting parameters (0.140 μm). The best simultaneous fit for both polarizations obtained for this model with gradually increasing twist model is shown as solid line in Figure 5 ($\delta_{\text{bulk}} = 9.5°$, $\varepsilon_{\text{II}} = 2.06$, $\varepsilon_{\perp} = 2.53$).

The fitting parameters are listed in Table I. As one can see the positions of the wave-guide modes now coincide quite well with the measurements. However, the simulated wave-guide modes are sharper than the experimental data. Misalignments in the sample broadens the resonance lines and at least for the fit in Figure 5 (*p* polarization) the discrepancy of the fit and experiment may be explained by these effects. In *s* polarization however, there is a systematic deviation in strength of one of each wave-guide doublet corresponding to positive electric field (the dips at 35, 41, 46, 51 and 56 degree). We tried to improve the fit by considering other possible profiles within the boundary layer, *e.g.*, nonlinear behavior of the twist angle, pretilt in the boundary layers or biaxiality of the optical tensor in the SmC* phase. None of them could remove the discrepancy observed between fit and data in *s* polarization. It may be that a combination of these possibilities would lead to a better fit. Changes of the director profile of the bulk layer can be excluded due to the strong electric field of $E = 1.3 \times 10^4$ V/cm.

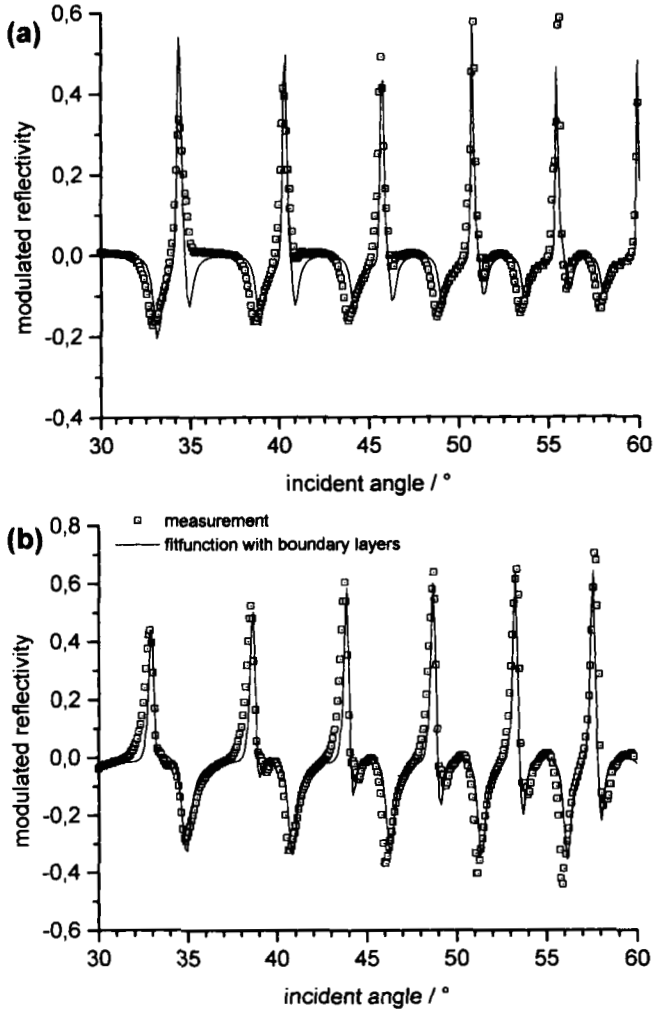

FIGURE 5 The same data as in Figure 3 fitted with the Chevron model including surface boundary layers (solid lines) for (a) *s* polarization and (b) *p* polarization. The thickness of the boundary layers is 140 nm. The fitting parameters are listed in Table I. The twist angle in the bulk is 9.5 degree.

We also measured the frequency dependence of the reorientation. Figure 6 shows the frequency dependence of the complex modulated reflectivity for *p* polarized light for the peak observed at an incident angle of 57.1 degree (see Fig. 3–*p* polarization). The amplitude of the modulated signal decreases as the frequency increases. As the frequency approaches the

TABLE I Parameters used for the fitting of the data. Parameters which were used as fitting parameters are printed bold face, the others were determined from the static measurements

glass	$\varepsilon = 2.296$			
gold	$\varepsilon = -12 + 1.1i$		$t = 43$ nm	
polyimide	$\varepsilon = 2.477$		$t = 29$ nm	
(a) liquid crystal (homogeneous switching model)	$\boldsymbol{\epsilon_{\parallel} = 2.53}$	$\boldsymbol{\epsilon_{\perp} = 2.06}$	$\boldsymbol{t = 4.225}$ μm	$\boldsymbol{\delta = 9.5°}$
(b) liquid crystal (with boundary layer)	$\boldsymbol{\epsilon_{\parallel} = 2.53}$	$\boldsymbol{\epsilon_{\perp} = 2.06}$	$\boldsymbol{t_{bulk} = 4.055}$μm $\boldsymbol{t_b = 0.140}$ μm	$\boldsymbol{\delta_{bulk} = 9.5°}$ $\boldsymbol{\delta_b = 9.5° \cdot t/t_b}$ $\boldsymbol{0 < t < t_b}$

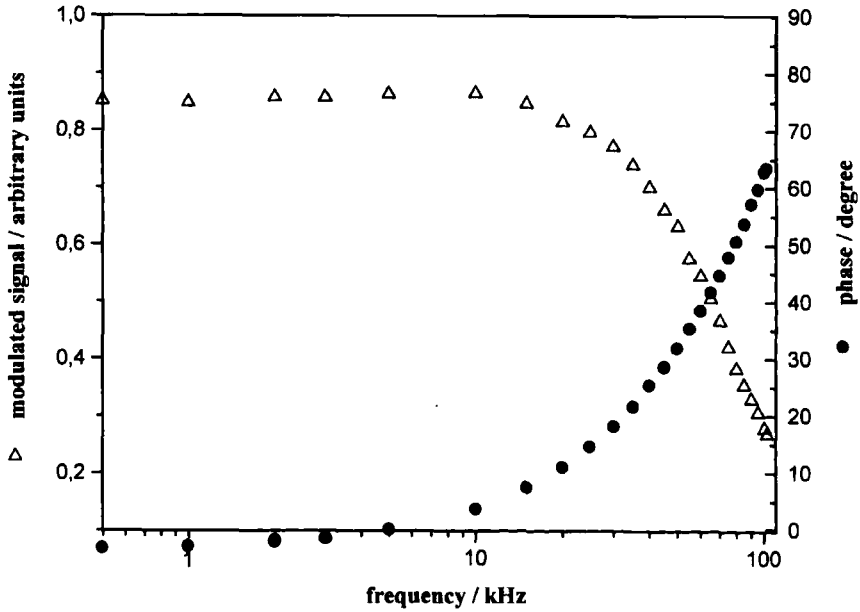

FIGURE 6 Frequency dependence of the modulated intensity for *p*-polarization (incident angle 57.1°). Open triangles represents the amplitude while the open circles depict the phase of the signal.

relaxation rate of the Goldstone mode, the liquid crystalline molecules cannot follow the applied electric field and the absolute value of the response drops to zero. At the same time the phase lag of the response is increasing from zero phase lag towards approximately 65 degree at 100 kHz.

CONCLUSION

Dynamic wave-guide spectroscopy is a useful tool for the determination of dynamic reorientation processes in liquid crystals. In accordance with other work the structure of the liquid crystal in the SmC* phase is well described by the Chevron model. The data could be consistently described with surface boundary layers reaching out approximately 0.14μm from the cell surface. In these boundary layers the switching dynamics is suppressed. The measured frequency dependence of the modulated signal shows a Goldstone-mode-like dynamics of the liquid crystalline mixture.

Acknowledgement

Support by the German Science foundation (DFG) within the project KR 1138/5 is highly acknowledged.

References

[1] S. J. Elston, J. R. Sambles and M. G. Clark, *J. Appl. Phys.*, **68**, 1242 (1990).
[2] S. J. Elston, *Liq. Cryst.*, **9**, 5769 (1991).
[3] F. Z. Yang and J. R. Sambles, *J. Opt. Soc. Am B*, **10**, 858 (1993).
[4] F. Z. Yang and J. R. Sambles, *Liq. Cryst.*, **13**, 1 (1993).
[5] F. Z. Yang, J. R. Sambles and G. W. Bradberry, *Liq. Cryst.*, **18**, 407 (1995).
[6] S. Ito, F. Kremer, T. Fischer and W. Knoll, *Mol. Cryst. Liq. Cryst.*, **264**, 99 (1995).
[7] M. Mitsuishi, S. Ito, M. Yamamoto and W. Knoll, *Appl. Phys. Lett.*, **69**, 2199 (1996).
[8] M. Mitsuishi, S. Ito, M. Yamamoto, T. M. Fischer and W. Knoll, *J. Appl. Phys.*, **81**, 1135 (1997).
[9] Z. Zhuang, N. A. Clark and M. R. Meadows, *Am. Phys. Soc.*, **45**, 6981 (1992).
[10] G. Pelzl, P. Kolbe, V. Preukschas, S. Diele and D. Demus, *Mol. Cryst. Liq. Cryst.*, **53**, 167 (1979).
[11] T. P. Rieker, N. A. Clark, G. S. Smith, D. S. Parmer, E. B. Sirota and C. R. Safinya, *Phys. Rev. Lett.*, **59**, 2658 (1987).
[12] M. H. Anderson, J. C. Jones, E. P. Raynes and M. J. Towler, *J. Phys. D.*, **24**, 338 (1991).
[13] L. Z. Ruan, J. R. Sambles and J. Seaver, *Liq. Cryst.*, **21**, 909 (1996).